Neutron and proton datafiles up to 150 MeV for ^{54}Fe, ^{56}Fe, ^{58}Ni and ^{60}Ni

A.J. Koning[1], O. Bersillon and J.-P. Delaroche

Service de Physique Nucléaire, CEA Bruyères-le-Châtel, BP 12, F-91680, Bruyères-le-Châtel, France

[1] **Present address**: *Netherlands Energy Research Foundation ECN, ECN - Nuclear Research, P.O. Box 1, 1755 ZG Petten, The Netherlands*

Abstract

We present 150 MeV neutron and proton transport datafiles for ^{54}Fe, ^{56}Fe, ^{58}Ni and ^{60}Ni. The high-energy part of the datafiles consists completely of results from model calculations, which are benchmarked against the available experimental data. These high-energy data are created with a code system built around the nuclear reaction codes ECIS96 and GNASH. The process from basic nuclear reaction physics up to the creation of MCNP-libraries is completely automized. For neutrons, the high energy data are automatically merged with an existing 20 MeV ENDF6-file. For protons, we construct completely new datafiles. The transport files cover light particles only, i.e. residual product yields are not included. In this report, we compare the evaluations with the few existing experimental data sets.

JEFF Room document
JEFF Specialists' Meeting on Intermediate Energy data,
June 18 1997, NEA Data Bank, Paris.

DRAFT VERSION

1 Introduction

Accelerator-based transmutation of waste, energy amplification, and medical isotope production as well as some new fusion concepts are examples of projects that drive the work on nuclear data above 20 MeV. Feasibility calculations of these systems, which include items as neutron and energy balance, the radiotoxicity of spallation products, damage and activation calculations, heavily rely on well-tested nuclear data, and the task of a nuclear data evaluator is to provide this information in a form that enables macroscopic transport and activation calculations.

There are basically two ways to provide a link between nuclear reaction physics and applied analyses. The first method is to perform the calculation of both microscopic nuclear reactions and macroscopic transport processes by one and the same computer code. HETC, LAHET and FLUKA [1] are well-known examples of intranuclear cascade codes that work according to this principle. The alternative method is to use nuclear model calculations, benchmark them with available experimental data and subsequently store the data into evaluated data files, using the ENDF6-format. If the necessary information stems from various reaction mechanisms, one or more computer codes based on dedicated nuclear models can be used to generate the data. One can also directly include experimental data in the datafile. The data evaluation method arguably enables the closest possible connection between nuclear reaction physics and practical applications. After processing, the data libraries can serve as input for deterministic or Monte-Carlo nuclear transport codes. Of course, since a few decades evaluated data files are already an important part of fission and fusion reactor research.

At present, both methods are regarded as complementary valuable approaches for analyses of accelerator-driven systems. The matching energy is around 150 MeV. Above this energy, pion production becomes important and the present ENDF6-format does not cover such reactions. Of course, the real problem is that the present transport codes (MCNP) are not yet extended with multi-particle abilities. Clearly, intranuclear cascade codes that handle both the cross section generation and the transport part for various types of particles should be used here. On the other hand, below 150 MeV, the predictive power of pre-equilibrium/statistical model codes such as GNASH [2] is superior [1] to intranuclear cascade codes for continuum reactions. Moreover, individual reaction mechanisms (giant resonances, coupled channels, etc.) constitute a relatively larger fraction of the reaction spectrum and require an individual, more sophisticated treatment. As a first step, we argue that a global calculation scheme for accelerator-driven systems should consist of a combination of intranuclear cascade codes above 150 MeV and evaluated data libraries for energies up to 150 MeV. We stress that even though the incident beam for several accelerator concepts is approximately 1 GeV, a detailed analysis of the energy region below 150 MeV is very important (neutron production, shielding, activation, etc.). Also, we feel that quality assurance, which has become quite an important issue in any working process, is more easily guaranteed for data libraries than for intranuclear cascade codes, which allow much freedom with input parameters.

In this paper, we present 150 MeV neutron and proton transport datafiles for ^{54}Fe, ^{56}Fe, ^{58}Ni and ^{60}Ni that have been created in a Bruyères-le-Châtel/ECN Petten collaboration. We will discuss the code system that was used to create the datafiles, some of the physics, and we give some comparisons between the datafile and experimental data.

2 The evaluation code system

Here we will briefly describe the code system [3] that produces the high-energy datafiles. The purpose of this code system is to automize calculations with several codes, and thereby the creation of their input files, that are necessary at various stages of the process. Hence, we automatically perform nuclear model calculations, store the results in an ENDF6-datafile, check the datafile and process it into multi-group or continuous energy format. The energy region for the nuclear model calculations runs from 20 MeV (or from threshold for protons) to 150 MeV. (We note that our set-up may also be suitable for incident energies below 20 MeV). The flow chart of the code system is given in Figs. 1-2. The advantage of our approach is that we only specify the desired calculations *once* after which a script takes care of all required calculations. This includes the nuclear reaction codes ECIS96 [4] and GNASH [2], the ENDF6-generator MINGUS3, the checking codes CHECKR, FIZCON, PSYCHE [5] and the processing code NJOY [6]. Basically, we start with an input file that specifies the nuclear model parameters and, in the case of neutrons, an existing 20 MeV datafile. Then, a shell script is submitted, and without any human interference we end up with a checked 150 MeV ENDF6-datafile and (for neutrons) a 150 MeV MCNP-library. The 20 MeV part of the neutron datafiles are taken from ENDF/B-VI.3.

3 Total, reaction and elastic cross sections

3.1 Optical model

For high-energy data evaluation, the optical model is of central importance. In the context of the present work, it has two purposes:

1. A "direct" application: It generates the total, total elastic and the total reaction cross section as well as the elastic angular distributions.

2. An "indirect" application: It is used for direct reaction calculations for discrete states, which can be done with DWBA for the (near-)spherical nuclei we are studying here, and it also generates the transmission coefficients that are used in the statistical model (Hauser-Feshbach) calculations.

In order to perform calculations without any unphysical discontinuities, optical models for the whole energy range of the datafile should, preferably, be used. Although we are primarily interested in incident energies above 20 MeV, optical potentials for low *outgoing* energies are required for spectrum calculations at any incident energy. When we have one optical model parametrization for the whole energy range, we can obtain both total and elastic cross sections varying smoothly with incident energy (see however Sec. 3.2) and smoothly varying results from GNASH.

With our interactive optical model tool ECISVIEW [7], we have constructed new phenomenological proton and neutron optical models for the energy range 0-200 MeV for all nuclei under study here. Figs. 3-10 show a comparison of our optical models with total cross sections and elastic angular distributions. The figures are in fact snapshots of ECISVIEW, and display the end result of the interactive parameter fitting procedure.

Future fine-tuning of the parameters is foreseen when the new total cross section measurements from Los Alamos [8] become available. For the functional form of the parametrization (we intend to publish the actual parameters for the iron and nickel isotopes later) that is required to obtain a single optical model parameter set over such a broad energy range we refer to [7]. Both the neutron and proton optical models incorporate relativistic kinematics. For the other outgoing channels we use global potentials, *i.e.* the deuteron potential of Lohr and Haeberli [9], the triton potential of Becchetti and Greenlees [10] and the alpha potential of Macfadden and Satchler [11]. All optical model calculations are done with ECIS96.

3.2 Storage in the datafile

The technical aspects of storing the data have been described in detail in Refs. [12, 13]. Here we restrict ourselves to stating that we cannot avoid some small discontinuities at 20 MeV in the neutron file. This stems from our (provisional) rule that we leave the existing 20 MeV neutron datafile untouched and that we have chosen to fine-tune our optical model to the experimental data and not to the low-energy datafile. This results in "jumps" in the total cross section of the order of one percent. For the moment, we expect this to be insignificant when the datafile is used in applications. Fig. 11 shows the resulting evaluated neutron total cross section for the four isotopes. We calculate and tabulate the total, total elastic and the total reaction cross section at every 1 MeV of incident energy.

Another point we wish to discuss is the elastic angular distribution. We have used tabular format for the presentation of the data (see [13] for a discussion on the use of tabular format vs. Legendre coefficients). For neutrons, we use angle steps of 1,2,3 and 4 degrees for angles up to 45, 90, 135 and 180 degrees, respectively: a total of 96 angles (the ENDF6-maximum is 100). In Fig. 12, the elastic angular distribution for the highest incident neutron energy (150 MeV) at backward angles for ^{56}Fe is shown, both for the original ECIS-calculation (with the cross section calculated at every degree) and the value that is actually tabulated in the datafile. It is clear that the difference is very small and that the elastic angular distributions can be accurately represented. For protons, we use the nuclear + interference expansion as discussed in [12].

4 Direct reactions to discrete states

4.1 DWBA calculations

Direct reactions to discrete states have been calculated with ECIS96 using the Distorted Wave Born Approximation (DWBA), using the aforementioned neutron or proton optical model. Deformation lengths for the first several MeV have been retrieved from the literature (Nuclear Data Sheets) and are appropriately transformed to deformation parameters, using the potential radius, for each component of the optical potential. The calculated DWBA cross sections are lumped and are included in the continuum spectrum as calculated by GNASH. The included discrete states for direct reactions for the four isotopes are given in Tables 1-4.

4.2 Storage in the datafile

The cross sections for the discrete states are included in the continuum spectra for inelastic scattering (MF6/MT5), using the Kalbach systematics [14] for the angular distribution. A possible future refinement is to store the inelastic cross sections to discrete states separately. This will also remove the problem of using the Kalbach systematics at the highest outgoing energies (where it should not be applied!) instead of the actual discrete angular distribution. Sensitivity studies may reveal whether this is a necessity.

5 Pre-equilibrium and compound reactions

The physics of the GNASH code has been extrensively describe in [2] so we don't repeat it here. We briefly mention the main topics of the calculation.

5.1 Pre-equilibrium reactions

In GNASH, angle-integrated pre-equilibrium cross sections are calculated with the exciton model of Kalbach [15]. For continuum angular distributions, the Kalbach systematics is used for all outgoing particles. Secondary pre-equilibrium emission is taken into account.

5.2 Level densities

We used the standard level density options of GNASH. For the pre-equilibrium part, the particle-hole level density of Williams is used. For compound nucleus reactions, we use the Ignatyuk formula [16], and we account for an appropriate matching of discrete levels and the continuum.

5.3 Compound reactions

We include a large number of possible reaction paths and take into account multiple particle evaporation until all final outgoing channels are closed. For the present evaluation, we included residual nuclei that were up to 7 protons and 11 neutron lighter than the target nucleus. Gamma-ray transmission coefficients were calculated using the Kopecky-Uhl model [17].

5.4 Storage in the datafile

The results of all spectrum calculations are stored in MF6/MT5 as yields and energy-angle distributions of outgoing particles (neutrons, protons, deuterons, tritons and alpha's) and photons (assumed isotropic). When combined with the (n(p),x) cross section of MF3/MT5, the double-differential spectra can be recovered. Recoils are not (yet) included. We tabulate the spectra at incident energy steps of 1 MeV below 30 MeV, 2 MeV steps between 30 and 50 MeV and 5 MeV steps between 50 and 150 MeV. We use an outgoing energy grid of 0.25 MeV for incident energies below 30 MeV, 0.5 MeV between 30 and 50 MeV, 0.75 MeV between 50 and 80 MeV and 1 MeV between 80 and 150 MeV.

6 Comparison with experimental data

The total, total elastic and the total reaction cross section and the elastic angular distributions that are stored in the datafile were automatically benchmarked when the optical model was constructed, see Figs. 3-10. All the other comparisons (i.e. of spectra) given in this report are done with results as retrieved directly from the datafile, i.e. for absolute safety we check the end product (and not the GNASH-output, although they should give the same results). Figs. 13-17 present comparisons for several reactions. To get an impression of the difference between datafiles, we have plotted (n,xn) and (p,xn) spectra for the four isotopes in Figs. 18-19. This demonstrates the well-known simple and weak mass dependence of continuum structureless spectra.

7 Conclusions

We have created 150 MeV neutron and proton transport datafiles for ^{54}Fe, ^{56}Fe, ^{58}Ni and ^{60}Ni. The high-energy part of the datafiles consists completely of results from model calculations, which are benchmarked against the available experimental data. The comparison between the datafiles and experimental data as given in this report gives an impression of the quality of the datafiles. Although there is obviously future work left regarding fine-tuning of several parts of the datafile, we argue that the representation of nuclear reaction information up to 150 MeV is already better than can be attained with intranuclear cascade codes. This is not surprising since we used dedicated model codes for different parts of the calculation and were able to fine-tune the input parameters of the model codes with experimental data. We realize however that sensitivity studies and comparisons with integral experiments should justify the effort to produce (more and more accurate) high-energy datafiles. The code system that we built around the nuclear reaction codes ECIS96 and GNASH is completely automized, from basic nuclear reaction physics up to the creation of MCNP libraries. This entails that when better nuclear reaction information becomes available (e.g. a better optical model, more precise pre-equilibrium cluster emission data etc.), this may immediately and very simply lead to an updated datafile. For neutrons, the calculated high energy data are automatically merged with an existing 20 MeV file. For the four isotopes considered here, we took the 20 MeV files of ENDF/B-VI-3 as basis. The ^{58}Ni data file has been used in a combined HETC/MCNP calculation [18]. For protons, we have constructed completely new datafiles. The latter may be used in future versions of MCNP [19] that can handle charged particles.

Acknowledgements

The authors are grateful to P.G. Young and M.B. Chadwick of Los Alamos National Laboratory for making the new LANL high-energy library available prior to publication.

References

[1] Proceedings of the NEA Specialist Meeting on *Intermediate Energy Nuclear Data: Models and Codes*, May 30-June 1 1994, Issy-les-Moulineaux, France.

[2] P.G. Young, E.D. Arthur and M.B. Chadwick, "Comprehensive nuclear model calculations: Introduction to the theory and use of the GNASH code", *Workshop on Nuclear reaction data and nuclear reactors* , April 15 - May 17 1996, Trieste, Italy.

[3] A.J. Koning, "Nuclear Data Evaluation for Accelerator-Driven Systems", *Second International Conference on Accelerator-Driven Transmutation Technologies and Applications*, June 3-7 (1996), Kalmar, Sweden.

[4] J. Raynal, *Notes on ECIS94*, CEA Saclay report (1994).

[5] C. Dunford, ENDF Utility Codes Release 6.10, IAEA report, IAEA-NDS-29, November 1995.

[6] R.E. MacFarlane,*The NJOY Nuclear Data Processing System, Version 91*, Report LA-12740-M, Los Alamos National Laboratory, 1994.

[7] A.J. Koning, J.J. van Wijk and J.-P. Delaroche,"ECISVIEW: A Graphical Interface for ECIS95", proceedings of the *NEA Specialists' Meeting on the Nucleon Nucleus Optical Model up to 200 MeV, Bruyères-le-Châtel*, November 13-15 1996. (WWW-address: http://db.nea.fr/html/science/om200/)

[8] F.S. Dietrich et al., "Recent measurements of neutron total cross sections on a wide range of targets from 5 to 600 MeV", contribution to the *International Conference on Nuclear Data for Science and Technology*, May 19-24 1997, Trieste, Italy.

[9] J.M. Lohr and W. Haeberli, Nuc. Phys. A232, 381 (1974).

[10] F.D. Becchetti and G.W. Greenlees, Nuc. Data Tables 17 (1976).

[11] L. Macfadden and G.R. Satchler, Nuc. Phys. 84, 177 (1966).

[12] A.J. Koning, *Requirements for an Evaluated Nuclear Data File for Accelerator-Based Transmutation*, NEA Data Bank Report NEA/NSC/DOC(93) 6.

[13] A.J. Koning and A. Hogenbirk, *High-energy nuclear data files: From ENDF-6 to NJOY to MCNP*, NEA Data Bank Report NEA/NSC/DOC(97) 8. (WWW-address: http://www.nea.fr/html/science/pt/iend/)

[14] C. Kalbach, "Systematics of continuum angular distributions: Extensions to higher energies", Phys. Rev. C37, 2350 (1988).

[15] C. Kalbach, "PRECO-D2: Program for calculating preequilibrium and direct reaction double differential cross sections", Los Alamos National Laboratory report LA-10248-MS (1985).

[16] A.V. Ignatyuk, G.N. Smirenkin and A.S. Tishin, Sov. J. Nucl. Phys. 21, 255 (1975).

[17] J. Kopecky and M. Uhl, Phys. Rev. C42, 1941 (1990).

[18] O. Bersillon et al., contribution to the *International Conference on Nuclear Data for Science and Technology*, May 19-24 1997, Trieste, Italy.

[19] R. Little et al., contribution to the *International Conference on Nuclear Data for Science and Technology*, May 19-24 1997, Trieste, Italy.

Spin/parity	Energy	Deformation length	Spin/parity	Energy	Deformation length
2+	1.408	0.86	4+	6.670	0.11
4+	2.538	0.31	3-	6.749	0.052
0+	2.561	0.31	4+	6.881	0.11
2+	2.959	0.49	3-	6.951	0.079
2+	3.166	0.24	3-	7.011	0.017
4+	3.295	0.22	3-	7.270	0.31
4+	3.834	0.37	2+	7.377	0.083
4+	4.048	0.14	3-	7.486	0.081
4+	4.265	0.31	3-	7.603	0.13
0+	4.290	0.15	3-	7.644	0.11
2+	4.579	0.17	4+	7.674	0.092
3-	4.781	0.46	3-	7.791	0.11
4+	4.949	0.16	3-	7.868	0.088
3-	5.148	0.079	3-	8.005	0.21
4+	5.232	0.14	3-	8.440	0.17
3-	5.534	0.13	3-	8.465	0.19
4+	5.657	0.12	4+	8.666	0.13
4+	5.703	0.14	3-	8.882	0.092
2+	5.806	0.083	3-	8.952	0.13
3-	5.907	0.052	3-	9.114	0.13
2+	5.956	0.030	3-	9.150	0.10
2+	6.192	0.057	3-	9.353	0.079
3-	6.341	0.45	3-	9.402	0.10
3-	6.401	0.70	3-	9.513	0.10
2+	6.429	0.20	3-	9.662	0.11
4+	6.484	0.15	3-	9.747	0.13
4+	6.607	0.11	3-	9.989	0.92

Table 1: Deformation lengths for direct reactions to discrete levels of ^{54}Fe.

Spin/parity	Energy	Deformation length	Spin/parity	Energy	Deformation length
2+	0.847	1.070	2+	4.730	0.230
4+	2.085	0.352	4+	4.860	0.179
2+	2.658	0.276	3-	5.062	0.207
2+	2.960	0.178	5-	5.106	0.872
4+	3.123	0.490	5-	5.122	0.220
6+	3.389	0.170	3-	5.195	0.200
2+	3.370	0.156	4+	5.266	0.230
2+	3.602	0.230	2+	5.535	0.230
2+	3.830	0.209	2+	6.480	0.253
4+	4.100	0.207	3-	6.500	0.281
4+	4.393	0.243	3-	7.000	0.281
2+	4.408	0.263	3-	7.500	0.314
4+	4.459	0.188	3-	8.000	0.314
3-	4.510	0.707	3-	8.500	0.281
4+	4.612	0.326	3-	9.000	0.281
4+	4.690	0.230			

Table 2: Deformation lengths for direct reactions to discrete levels of ^{56}Fe.

Spin/parity	Energy	Deformation length	Spin/parity	Energy	Deformation length
2+	1.454	0.900	4+	7.141	0.112
4+	2.459	0.350	3-	7.210	0.323
2+	3.038	0.242	2+	7.272	0.088
2+	3.263	0.306	3-	7.300	0.063
4+	3.620	0.246	3-	7.420	0.048
2+	3.898	0.111	3-	7.514	0.171
2+	4.108	0.063	2+	7.580	0.051
4+	4.299	0.127	4+	7.618	0.083
4+	4.405	0.329	3-	7.858	0.106
3-	4.475	0.708	4+	7.860	0.097
4+	4.757	0.403	3-	8.134	0.142
4+	5.438	0.151	3-	8.797	0.097
4+	5.472	0.080	3-	8.841	0.112
2+	5.749	0.048	4+	8.902	0.072
4+	5.766	0.086	3-	9.012	0.056
2+	5.906	0.115	3-	9.304	0.065
3-	6.312	0.128	3-	9.379	0.106
2+	6.417	0.068	4+	9.436	0.071
4+	6.460	0.098	3-	9.458	0.082
2+	6.475	0.065	4+	9.588	0.052
2+	6.569	0.056	4+	9.632	0.080
2+	6.752	0.141	3-	9.672	0.121
3-	6.854	0.296	3-	9.835	0.083
2+	6.983	0.116	3-	9.870	0.076
4+	7.051	0.090	3-	9.929	0.061
4+	7.068	0.086	3-	9.956	0.071
3-	7.111	0.079			

Table 3: Deformation lengths for direct reactions to discrete levels of ^{58}Ni.

Spin/parity	Energy	Deformation length	Spin/parity	Energy	Deformation length
2+	1.331	1.178	5-	5.010	0.362
2+	2.156	0.136	2+	5.100	0.326
0+	2.290	0.082	2+	5.260	0.453
4+	2.502	0.575	3-	5.390	0.222
2+	3.119	0.231	3-	5.600	0.281
3-	3.130	0.408	2+	5.800	0.186
2+	3.310	0.227	5-	5.980	0.159
4+	3.671	0.299	3-	6.160	0.326
3-	4.042	0.951	2+	6.340	0.208
4+	4.300	0.195	3-	6.530	0.172
2+	4.500	0.163	4+	7.000	0.285
3-	4.530	0.272			

Table 4: Deformation lengths for direct reactions to discrete levels of ^{60}Ni.

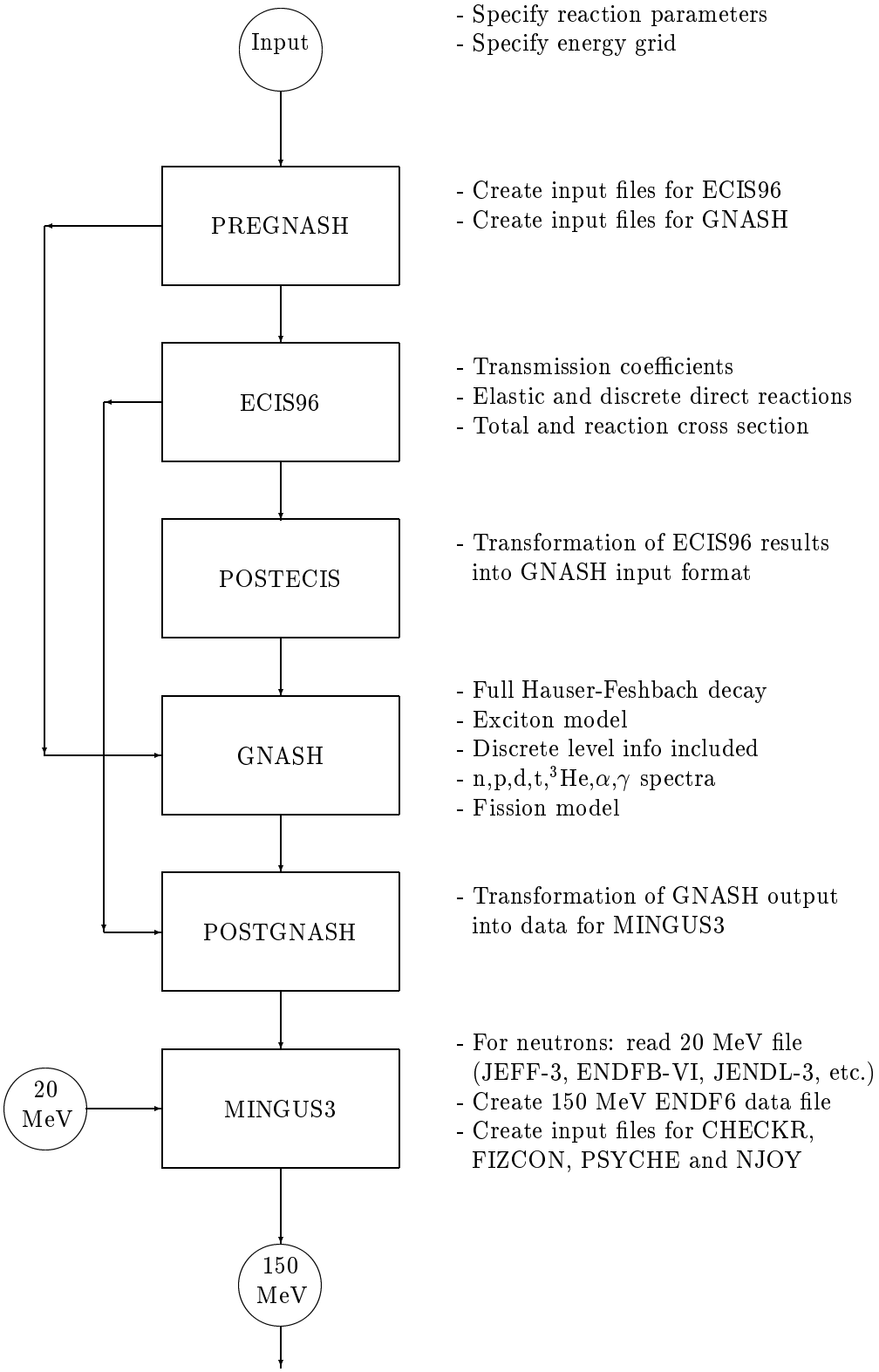

Figure 1: Flow chart of the evaluation code system: Part 1

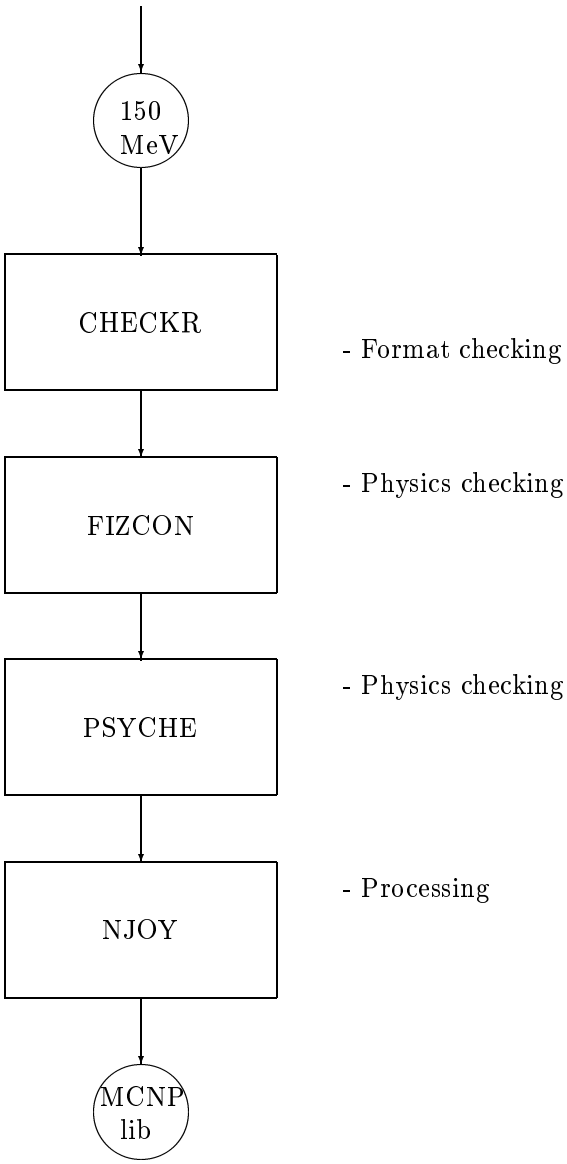

Figure 2: Flow chart of the evaluation code system: continued

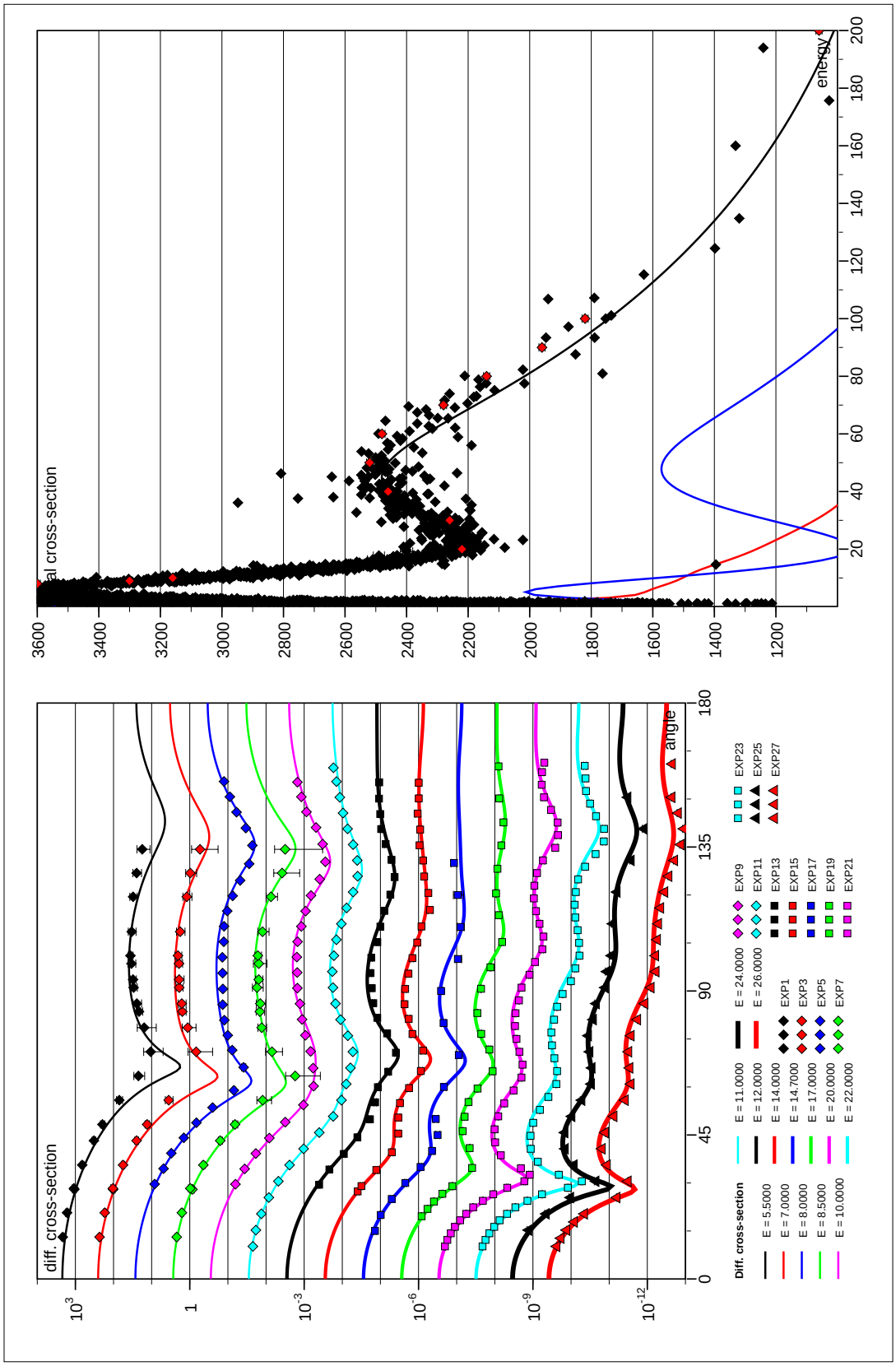

Figure 3: 0-200 MeV neutron optical model for ^{54}Fe.

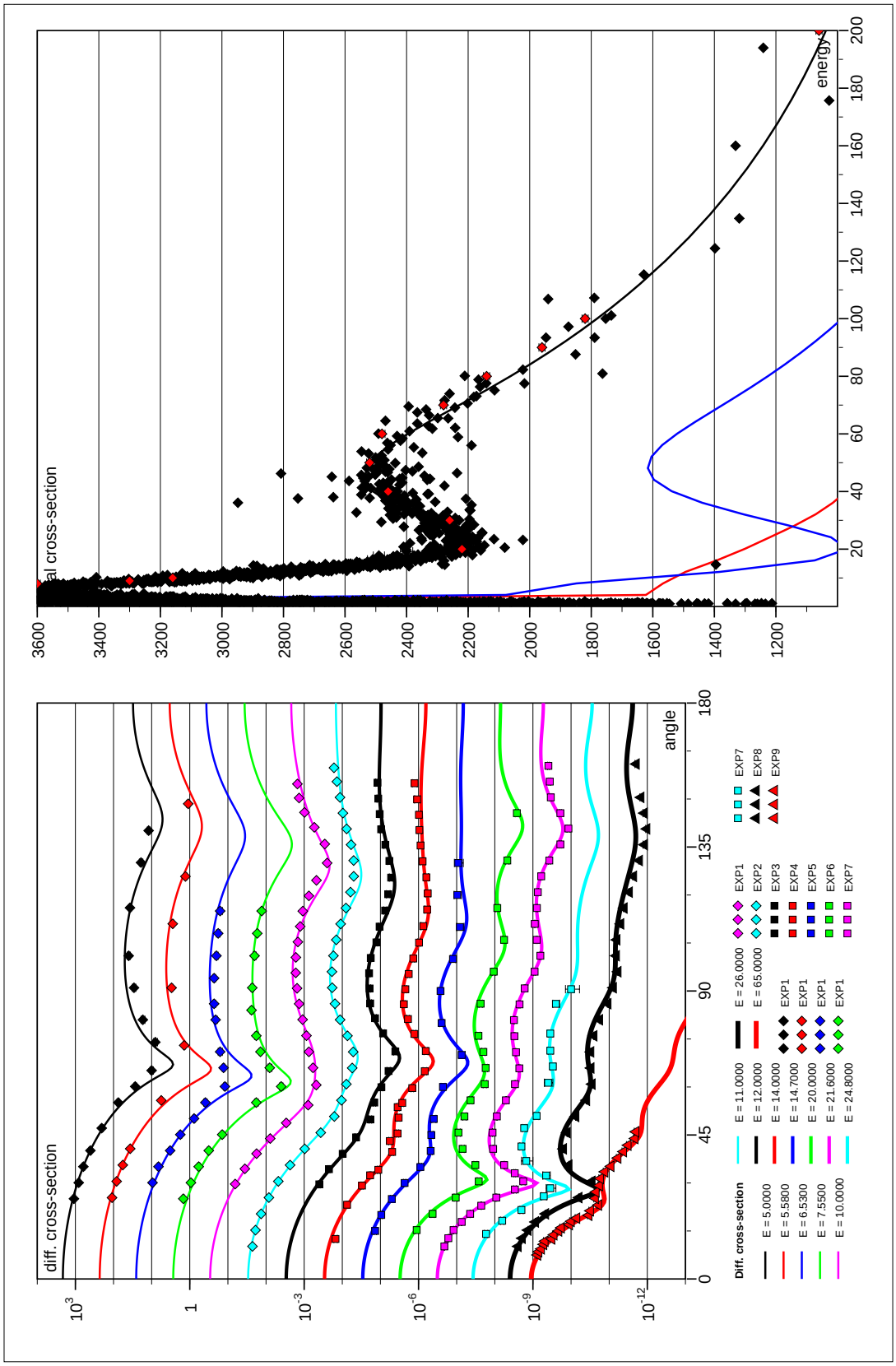

Figure 4: 0-200 MeV neutron optical model for ^{56}Fe.

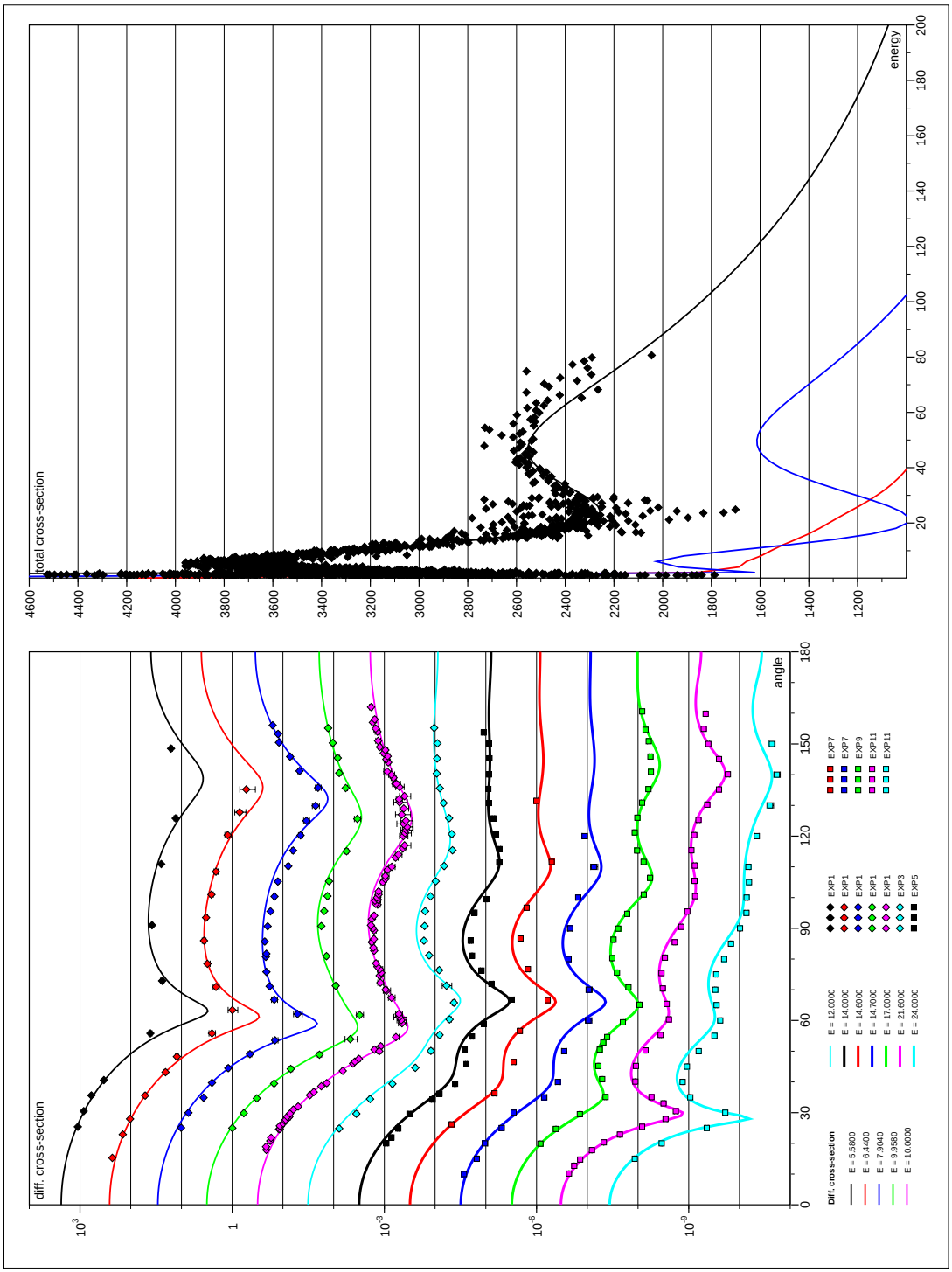

Figure 5: 0-200 MeV neutron optical model for ^{58}Ni.

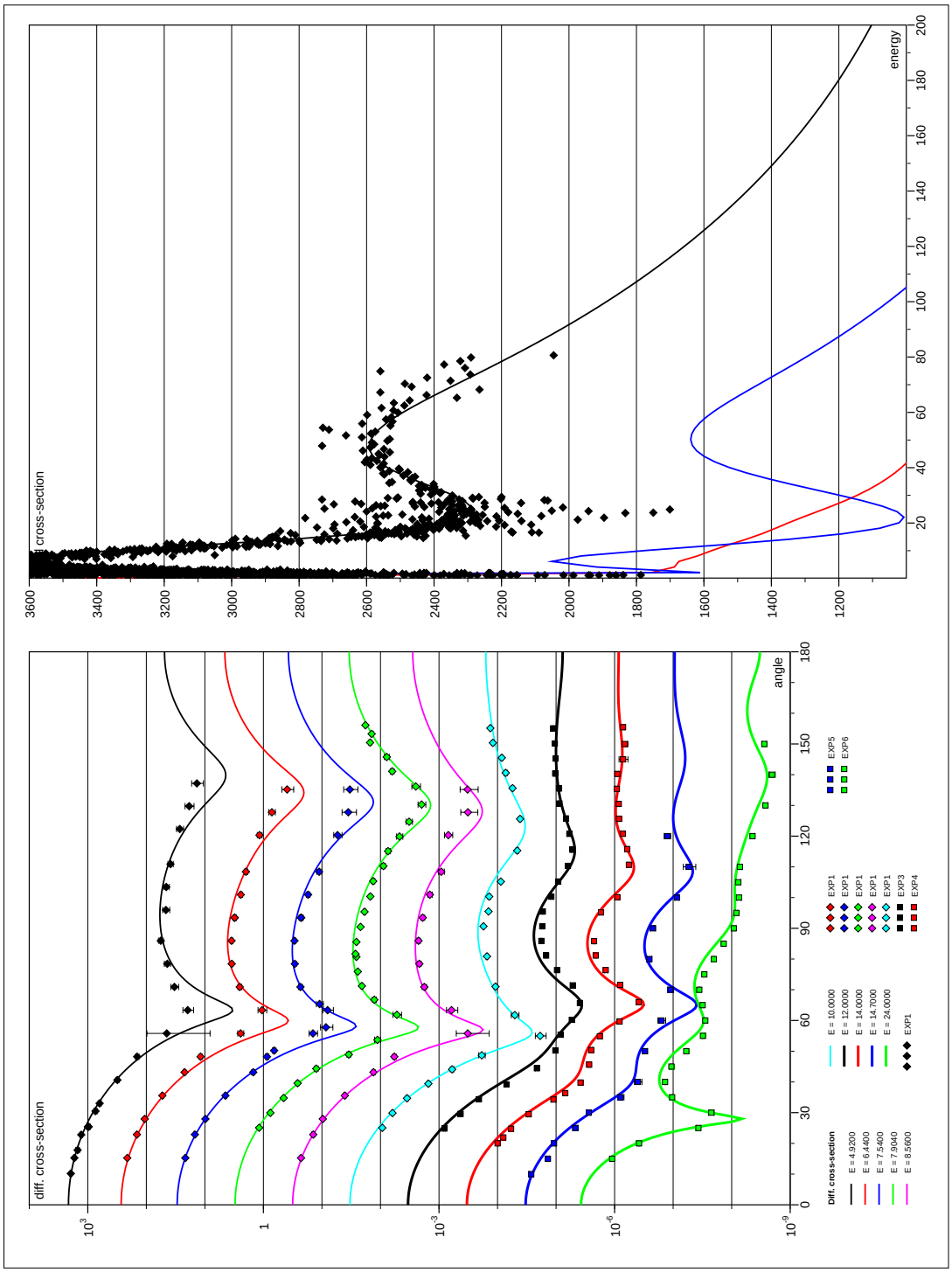

Figure 6: 0-200 MeV neutron optical model for ^{60}Ni.

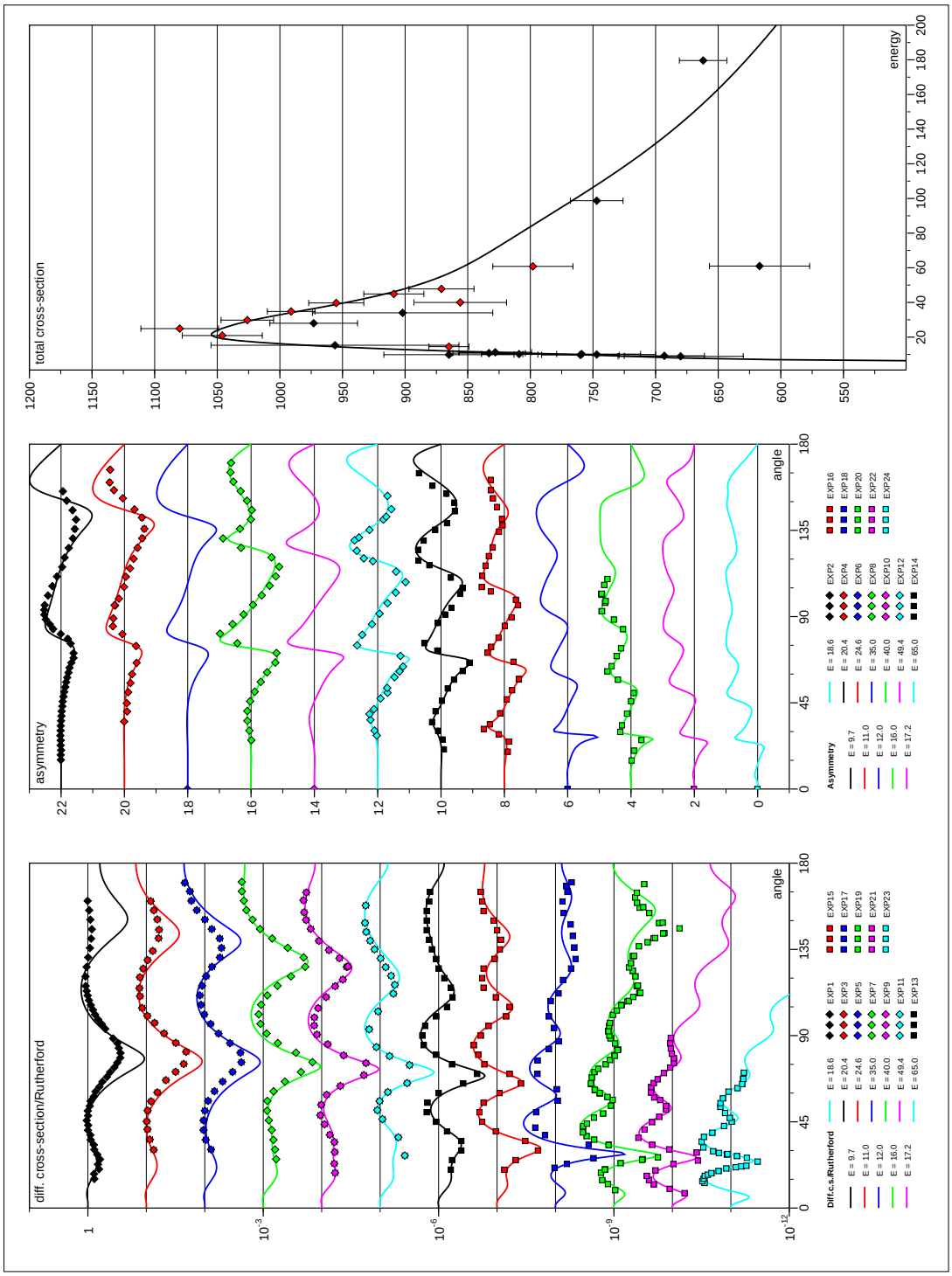

Figure 7: 0-200 MeV proton optical model for ^{54}Fe.

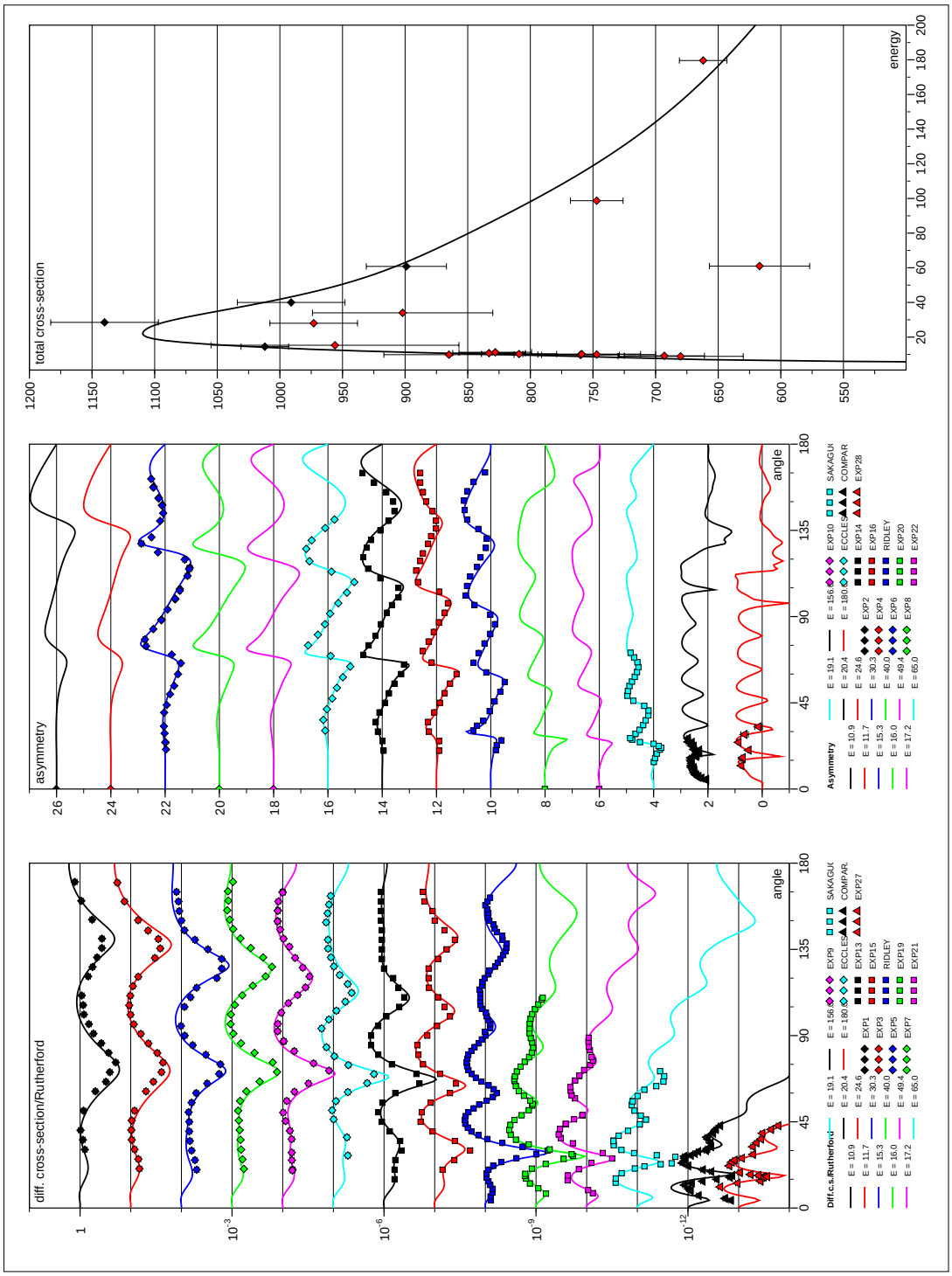

Figure 8: 0-200 MeV proton optical model for ^{56}Fe.

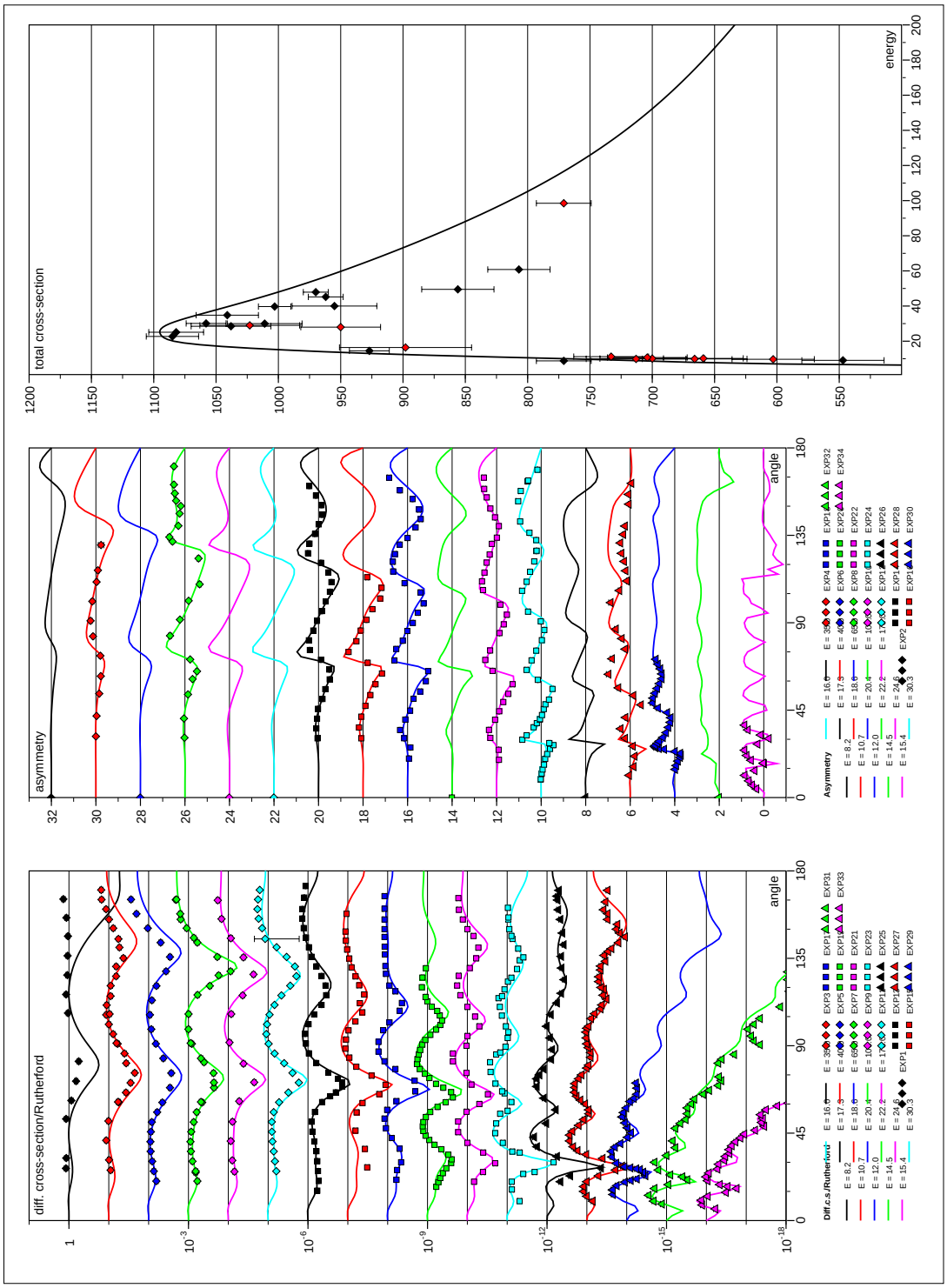

Figure 9: 0-200 MeV proton optical model for ^{58}Ni.

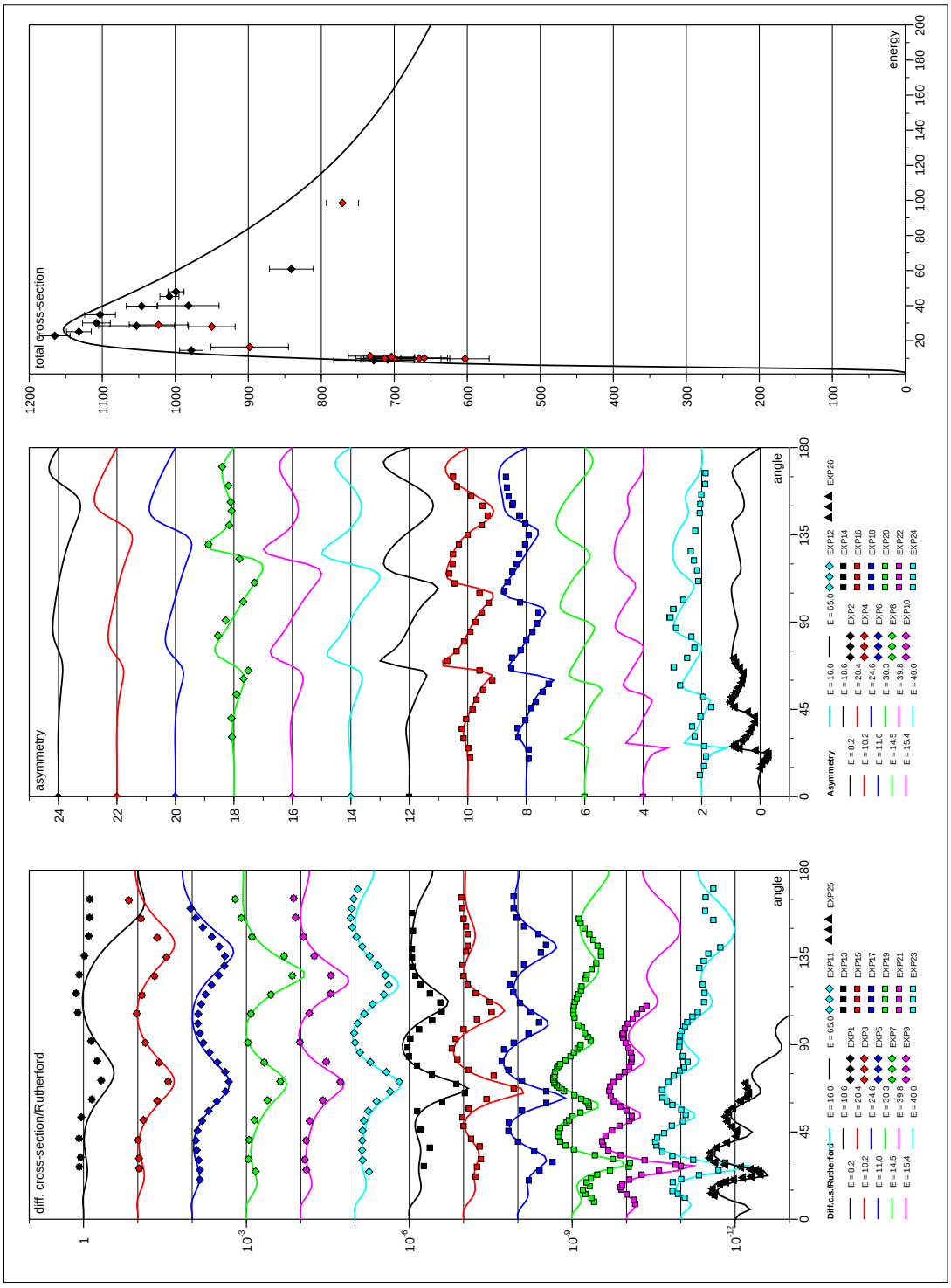

Figure 10: 0-200 MeV proton optical model for ^{60}Ni.

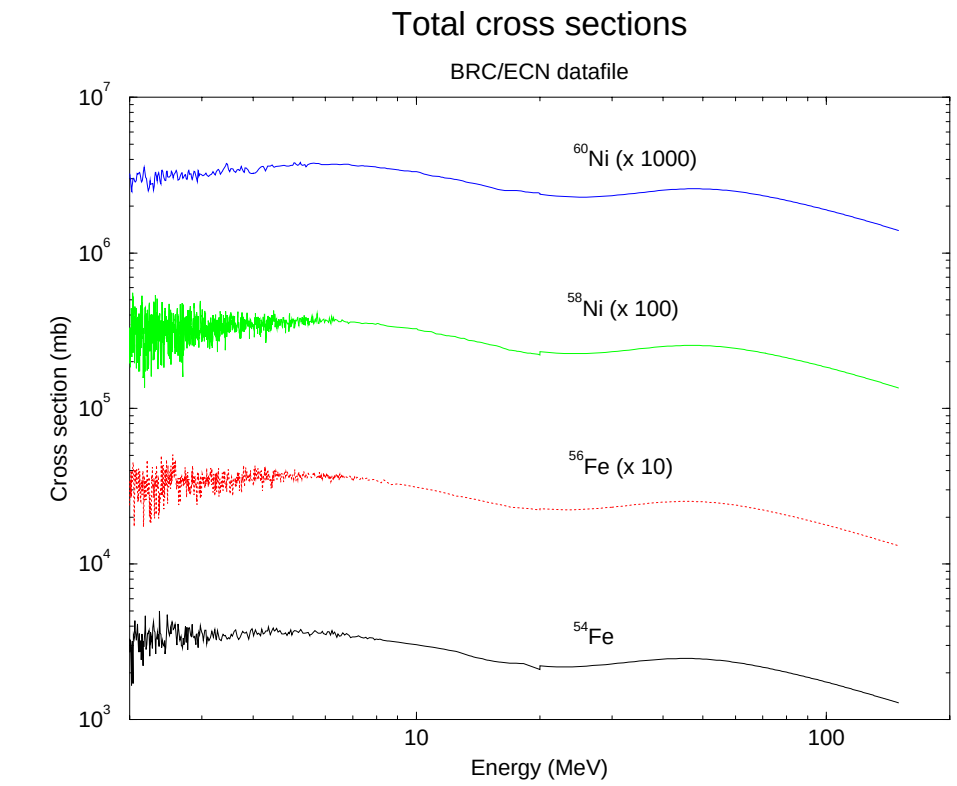

Figure 11: Total neutron cross section for the four isotopes of the BRC/ECN data library.

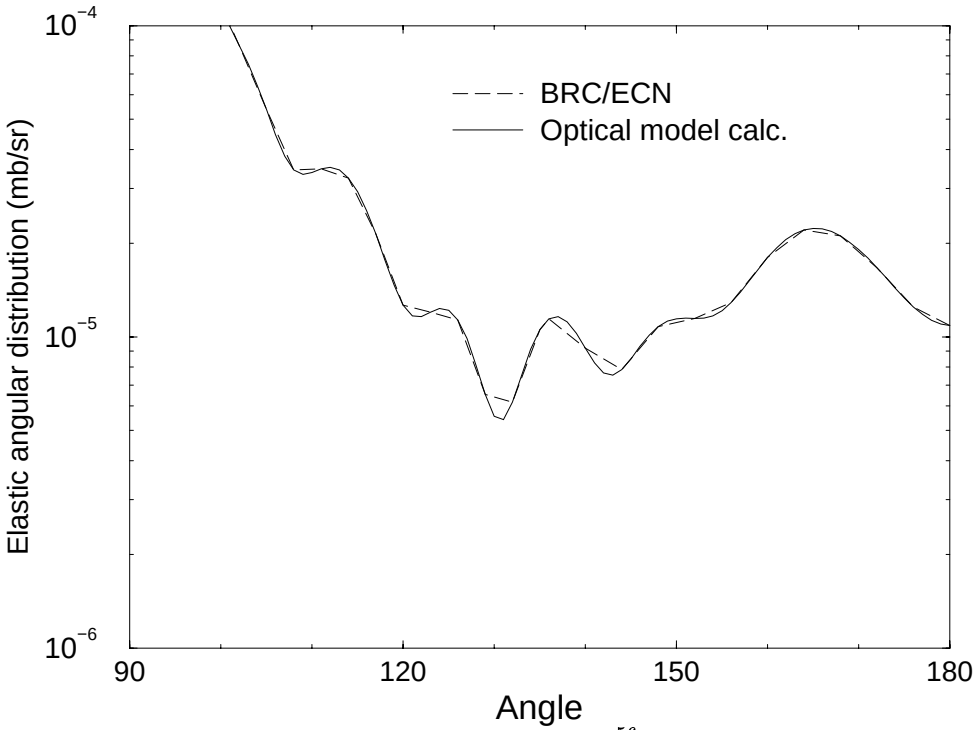

Figure 12: 150 MeV neutron elastic scattering on ^{56}Fe: Comparison between optical model calculation and the corresponding values as tabulated in the BRC/ECN datafile.

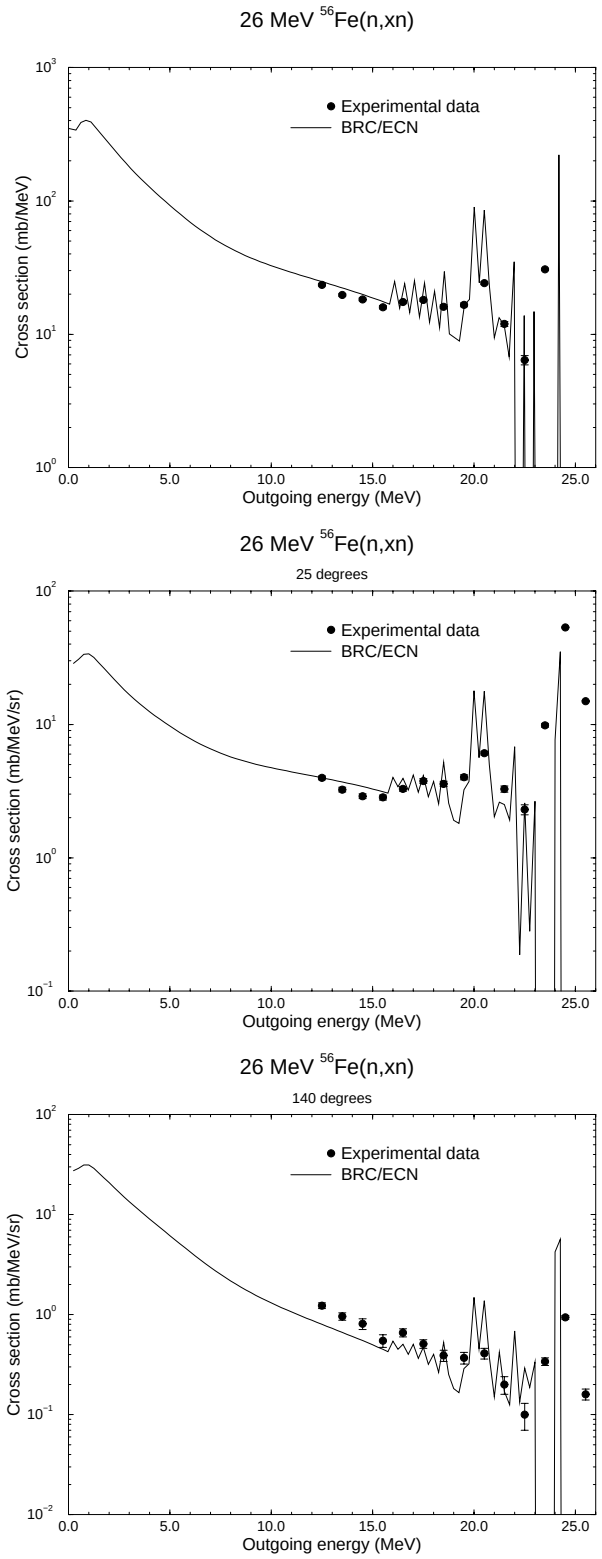

Figure 13: 26 MeV (n,xn) on ^{56}Fe: Comparison between BRC/ECN datafile and experimental data, (a) Angle-integrated, (b) 25 degrees, (c) 140 degrees.

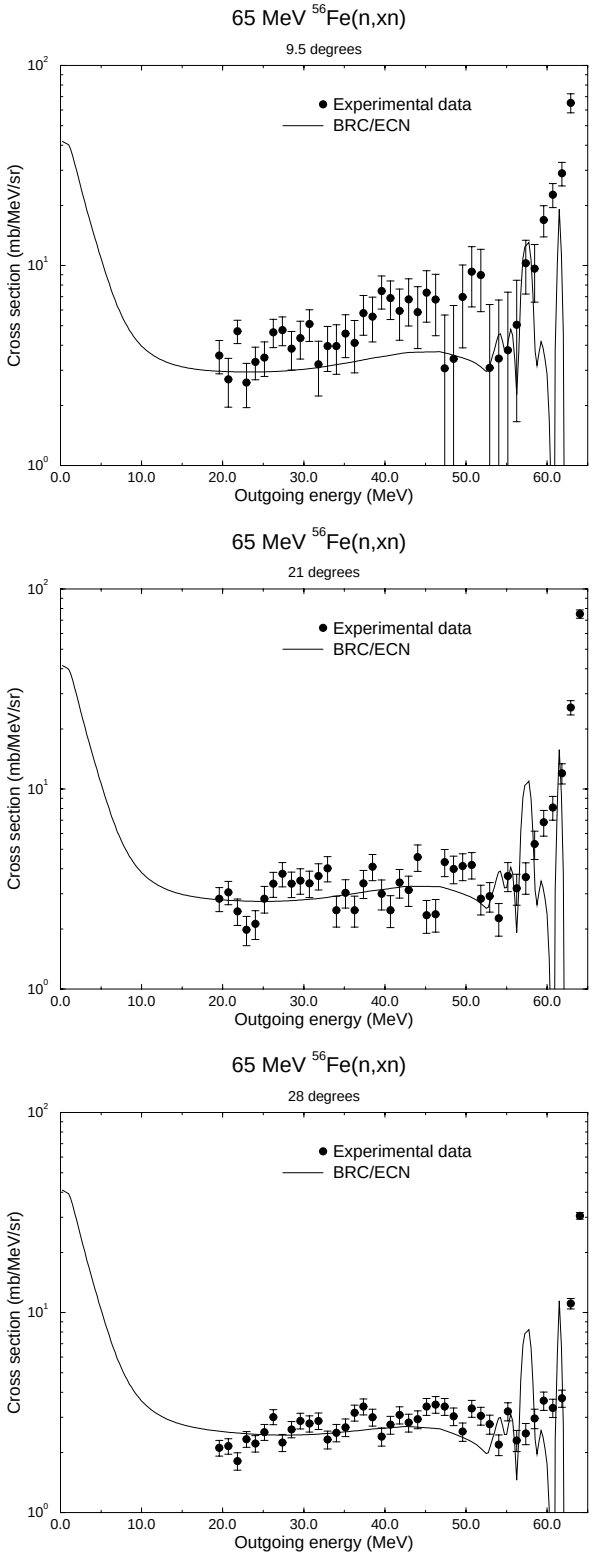

Figure 14: 65 MeV (n,xn) on ^{56}Fe: Comparison between BRC/ECN datafile and experimental data, (a) 9.5 degrees (b) 21 degrees, (c) 28 degrees.

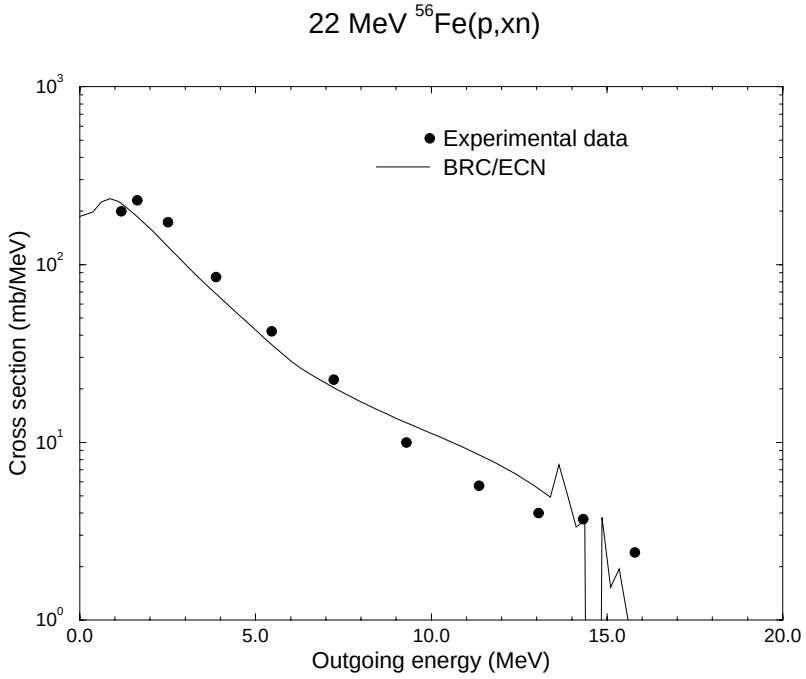

Figure 15: Angle-integrated cross section for 22 MeV (p,xn) on ^{56}Fe: Comparison between BRC/ECN datafile and experimental data.

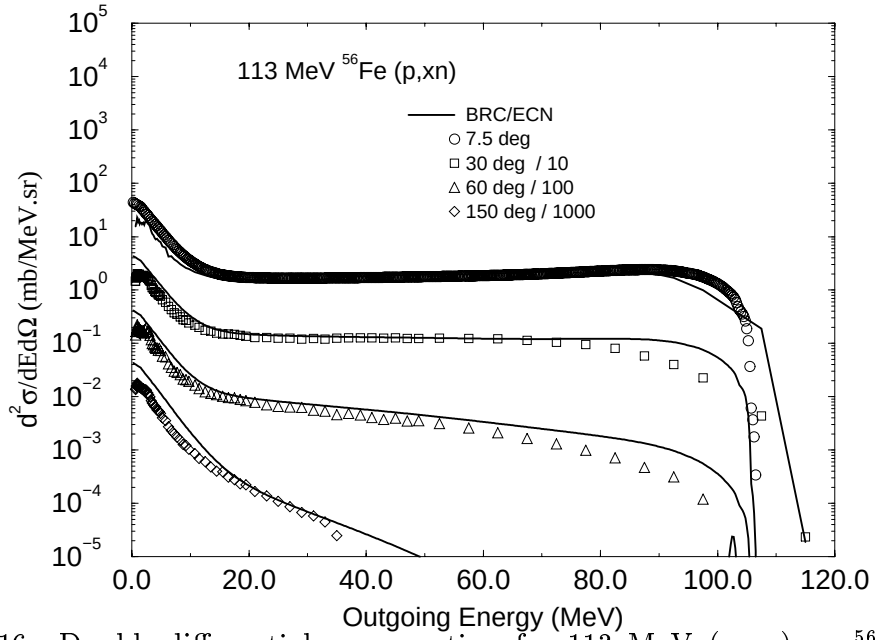

Figure 16: Double-differential cross section for 113 MeV (p,xn) on ^{56}Fe: Comparison between BRC/ECN datafile and experimental data.

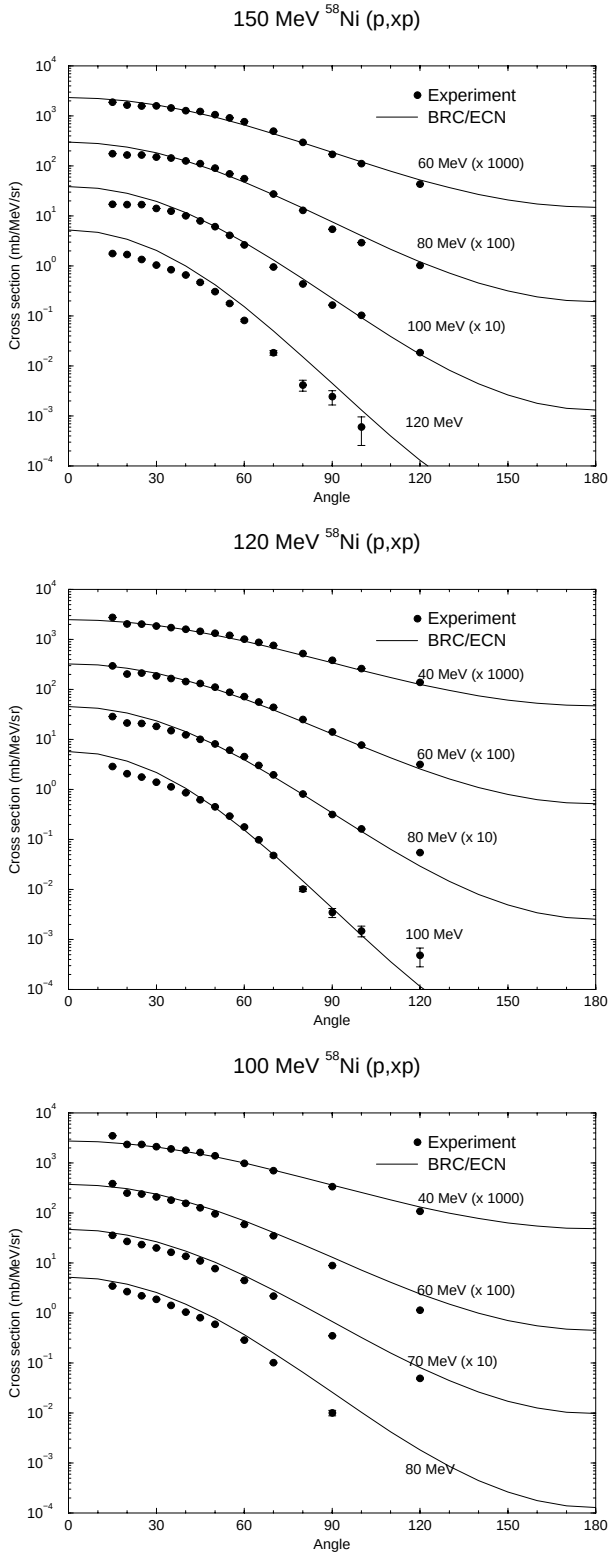

Figure 17: (p,xp) on ^{58}Ni: Comparison between BRC/ECN datafile and experimental data for incident energies at, (a) 150 MeV (b) 120 MeV, (c) 100 MeV at several outgoing energies.

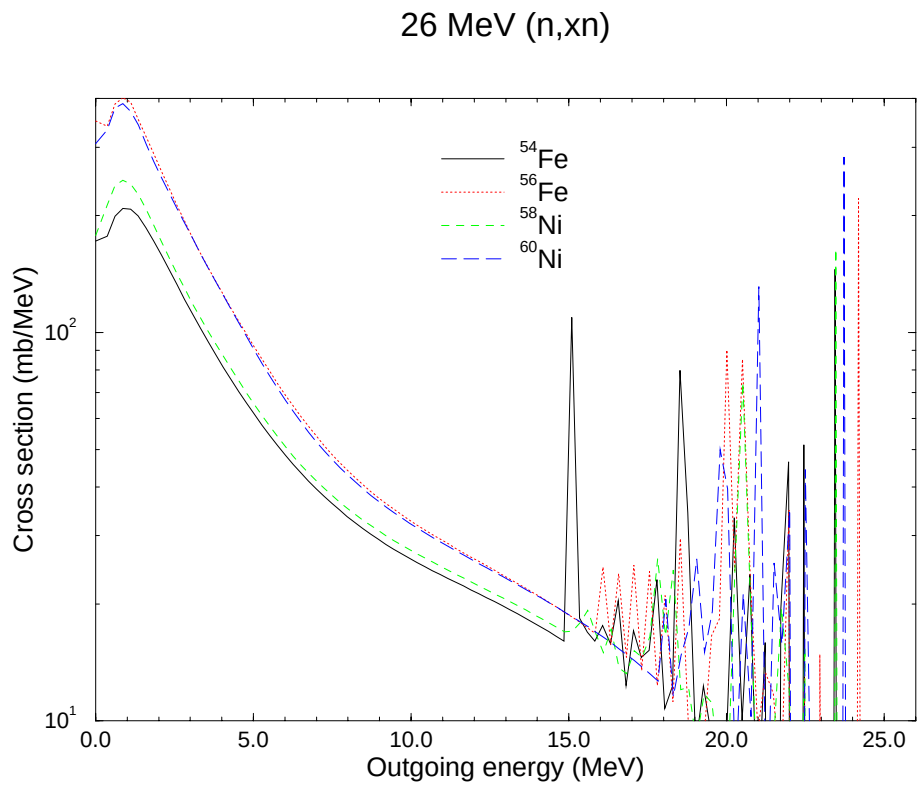

Figure 18: 26 MeV (n,xn) angle integrated cross section: Comparison between the four datafiles.

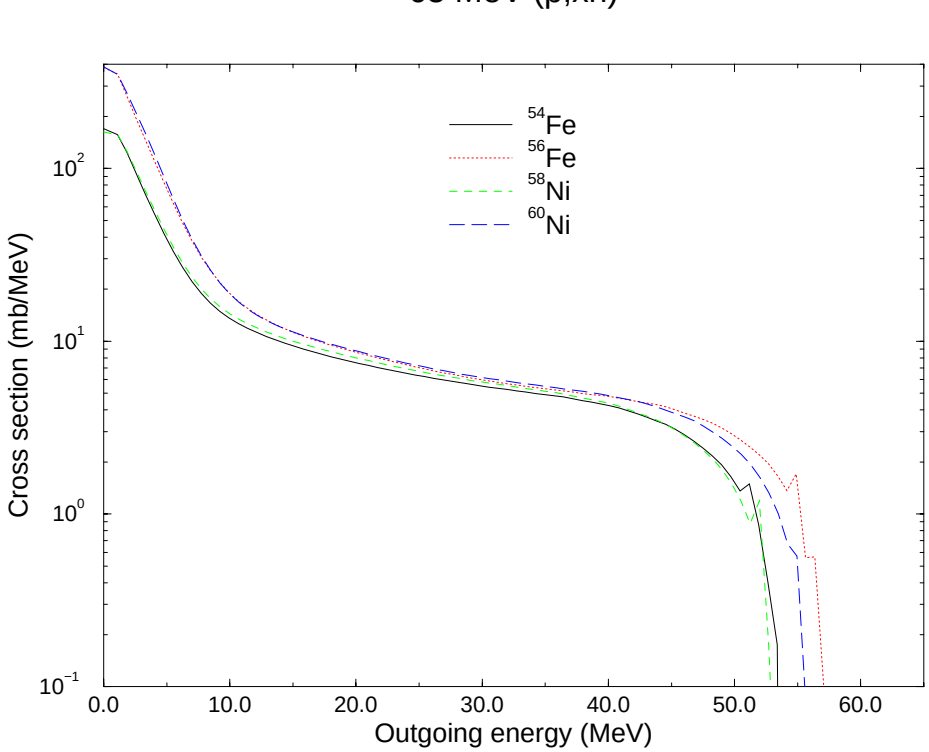

Figure 19: 65 MeV (p,xn) angle integrated cross section: Comparison between the four datafiles.